

Thickness of the left atrial wall surrounding the left atrial appendage orifice

Katarzyna Słodowska MD^{1,2} | Jakub Hołda MD^{1,2} | Damian Dudkiewicz MPT^{1,2} |
 Karolina Malinowska MSc^{1,2} | Filip Bolechała MD, PhD^{2,3} | Paweł Kopacz MD^{2,3} |
 Mateusz Koziej MD, PhD, DSc^{1,2} | Mateusz K. Hołda MD, PhD, DSc^{1,2}

¹Department of Anatomy, Heart Embryology and Anatomy Research Team, Jagiellonian University Medical College, Cracow, Poland

²Division of Cardiovascular Sciences, The University of Manchester, Manchester, UK

³Department of Forensic Medicine, Jagiellonian University Medical College, Cracow, Poland

Correspondence

Mateusz K. Hołda, MD, PhD, DSc,
 Department of Anatomy, Heart Embryology and Anatomy Research Team, Jagiellonian University Medical College, Kopernika 12, 31-034 Kraków, Poland.
 Email: mkh@onet.eu

Abstract

Introduction: The aim of this study was to investigate the thickness of the left atrial wall surrounding the left atrial appendage (LAA) orifice.

Methods and Results: The tissue thickness around the LAA orifice was measured at four points (superior, inferior, anterior, and posterior) in 200 randomly selected autopsied human hearts. The thickest tissue was observed at the anterior point (3.17 ± 1.41 mm), followed by the superior (2.47 ± 1.00 mm), inferior (2.22 ± 0.80 mm) and posterior (2.22 ± 0.83 mm). The chicken wing LAA type was associated with the lowest thickness at the superior point compared to the cauliflower and arrowhead shapes ($p = .024$). In hearts with an oval LAA orifice, the atrial wall was significantly thicker in all points than in specimens with a round LAA orifice ($p > .05$). Both the LAA orifice anteroposterior diameter and orifice surface area were negatively correlated with the tissue thickness in the anterior ($r = -.22$, $p = .004$ and $r = -.23$, $p = .001$) and posterior points ($r = -.24$, $p = .001$ and $r = -.28$, $p = .005$). Endocardial surface roughness was commonly in the inferior pole of the LAA orifice (75.5% of cases), while they are much less prevalent in other sectors around the orifice (anterior: 17.5%, superior: 4.0%, and posterior: 1.5%).

Conclusions: Although a significant heterogeneity in the atrial wall thickness around the LAA orifice was observed, the thickness in the respective points is quite conservative and depends only on LAA orifice size and shape, as well as LAA body shape. Thin atrial wall and endocardial surface roughness might challenge invasive procedures within this region.

KEYWORDS

ablation, atrial fibrillation, cardiac anatomy, LAA shape, left atrial appendage occlusion, left atrial wall, left atrium, tissue thickness

1 | INTRODUCTION

The left atrial appendage (LAA) is the irregular and highly trabeculated vestige of the primal embryonic left atrium that develops during early gestation.^{1–3} The LAA is connected to the left

atrium via a relatively narrow orifice.⁴ These features of the LAA, together with the disturbed blood flow that may occur in patients with atrial fibrillation, predispose to thrombogenesis within the LAA and consequent cardioembolic stroke.⁵ Approximately 90% of thrombi in patients with nonvalvular atrial fibrillation derive

from LAA.⁶ One of the well-recognized stroke prevention strategies is LAA mechanical exclusion.⁷ However, as with any intravascular intervention, LAA occlusion is burdened with some complications. The most severe include: perforation, pericardial effusion, device thrombus, and even procedure-related strokes.⁸ Various LAA properties, including the body type (shape and size) and LAA orifice geometry, are related not only to the increased thrombogenicity of the appendage but also to the success rate and durability of procedures targeted to the LAA.^{9,10}

The LAA has been progressively recognized in the initiation and maintenance of atrial tachyarrhythmias.^{11–13} Several LAA features might predispose to its arrhythmogenicity. First, the trabeculated muscle network within the LAA body generates areas of slow conduction, conduction block, and can initiate re-entrant circuits.¹⁴ Second, the LAA orifice interferes with the left atrial musculature, disturbing it and thus producing significant tissue anisotropy that results in electrophysiological non-heterogeneity.¹² Moreover, the LAA orifice is entwined by Bachmann bundle final fibers, and this connection with the LAA has been recognized in the initiation and maintenance of atrial fibrillation.¹⁵ In the last decade, the linear ablations at the base of the LAA or within the LAA or circumferential isolation of the LAA orifice are gaining popularity.^{12,13,16} Although the LAA electrical isolation is considered relatively safe, it may be challenging. The procedure is difficult and requires a complex mapping with the main concerns related to the LAA perforation during ablation. Nevertheless, no definite data exist on the optimal ablation energy and strategy to minimize this risk.¹⁷

Both the LAA mechanical exclusion and electrical isolation procedures affect not only the body of the LAA but also the surrounding rim of the left atrial wall. Therefore, in this study, we have aimed to evaluate the thickness of the left atrial wall surrounding the LAA orifice and to find associations between wall morphometric characteristics and the LAA type, presence of left lateral ridge, as well as the left-sided pulmonary venous drainage configuration. Providing such data will increase the anatomical knowledge and thus contribute to increased safety and efficiency of percutaneous procedures targeted to the LAA.

2 | MATERIALS AND METHODS

This current study was conducted at the Department of Anatomy at the Jagiellonian University Medical College. The study was conducted according to the principles expressed in the 1975 Declaration of Helsinki and was approved by the Bioethical Committee of the Jagiellonian University in Cracow, Poland (No. 1072.6120.4.2020).

2.1 | Study population

We have investigated 200 randomly selected autopsied human hearts (Caucasian) of both sexes (25.0% females). The mean age of donors was 46.6 ± 19.1 years, mean body weight and body height were 78.3 ± 14.1 kg and 1.71 ± 0.1 m, respectively and the mean body mass index (BMI) was 26.5 ± 4.8 kg/m². Hearts were collected during routine forensic medical autopsies executed at the Department of Forensic Medicine, Jagiellonian University Medical College in Cracow, Poland. Study exclusion criteria comprise past cardiac surgery, heart grafts, previous heart trauma, evident severe macroscopic pathologies revealed during an autopsy, vascular or cardiac anatomical defects, and macroscopic signs of cadaver decomposition. There were no donors with either a history of persistent atrial fibrillation or a thrombus identified in the LAA during autopsy among studied cases.

2.2 | Dissection, observations, and measurements

Hearts were dissected from the chest cavity in a routine manner. Then, all samples were inspected, washed out of excess blood, weighed, and afterward fixed in a 10% paraformaldehyde buffered solution until the time of the next observations and measurements. After sample preservation, the shape of the LAA was classified according to the previously established three-type classification system (Type I—the cauliflower: compact LAA body with a limited length, a variable number of lobes and without obvious bends, Type II—the chicken wing: a substantial bend in the proximal or middle part of the dominant lobe, Type III—the arrowhead: dominant lobe of substantial

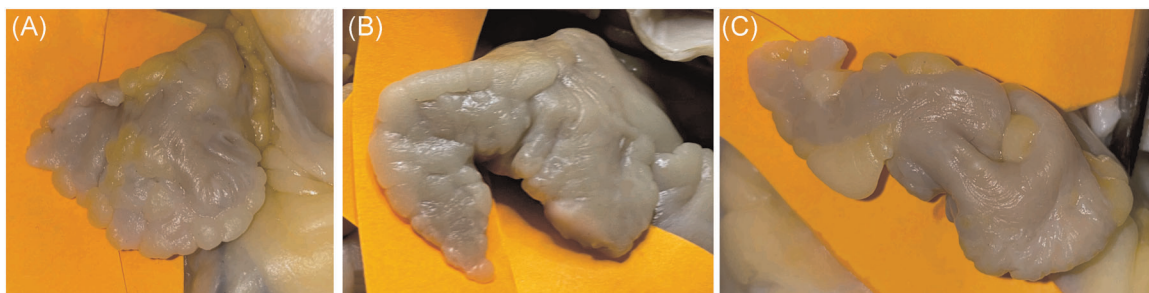


FIGURE 1 Photographs of cadaveric heart specimens showing different types of the left atrial appendage (LAA): (A) cauliflower, (B) chicken wing, (C) arrowhead

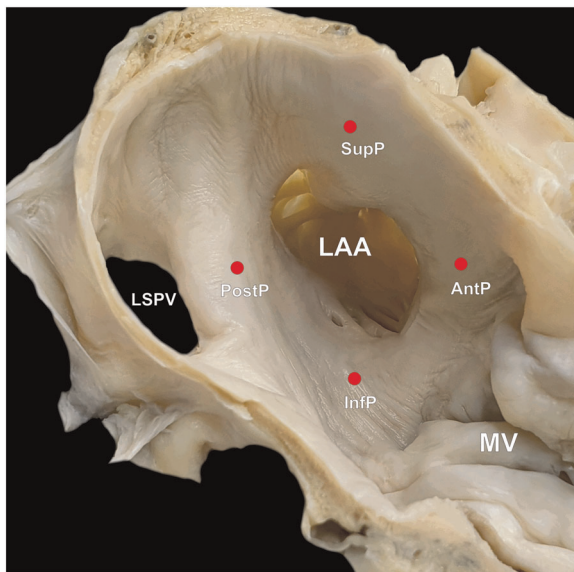


FIGURE 2 Photograph of a cadaveric heart specimen showing left atrial appendage (LAA) orifice with marked points of the cross-section, which allowed us to measure left atrial wall thickness. SupP—superior point (at the left atrium roof); InfP—inferior point (at the atrio-ventricular sulcus); AntP— anterior point (at the mitral valve [MV] annulus); PostP—posterior point (at the left-sided pulmonary vein ostia). LSPV, left superior pulmonary vein

length, LAA body without obvious bends) (Figure 1).¹⁸ Next, the left atrium was opened to expose the postero-lateral region of the left atrium and the LAA orifice to execute further observations and measurements. Both the transverse diameter (parallel to the mitral valve annulus) and the anteroposterior diameter (perpendicular to the mitral valve annulus) of the LAA orifice were measured. The shape of the LAA orifice was classified as oval or round, and the LAA orifice area was calculated as described above.¹⁸ The occurrence of any additional structures (crevices, diverticula, trabeculae, or tissue bridges) around the LAA orifice was documented. The presence of the left atrial ridge (defined as a prominent fold of tissue located between the left-sided pulmonary vein ostia and the LAA orifice) was also noted.¹⁹ We also investigated variations in the left-sided pulmonary vein ostia. Finally, the left atrial wall around the LAA orifice has been cut (3 mm from the LAA orifice edge) at four points (Figure 2) to obtain a cross-section which allowed us to measure the total wall thickness of the left atrium (endocardium, myocardium, and epicardium with adipose tissue):

- superior point—at the left atrium roof,
- inferior point—at the atrio-ventricular sulcus,
- anterior point—at the mitral valve annulus,
- posterior point—at the left-sided pulmonary vein ostia (Figure 2).

All linear measurements were conducted with 0.03-mm precision electronic calipers (YATO, YT-7201, Poland). To reduce human bias, all measurements were recorded by two independent investigators. If results between the two researchers varied by more

than 10%, both measurements were repeated. The mean of the two new values was calculated and reported as the final value.

2.3 | Statistical analysis

Data are shown as mean values with corresponding SDs (\pm SD) or determining percentages. To determine if the quantitative data were normally distributed, the Shapiro-Wilk test was used. Levene's test was performed to verify a relative homogeneity of variance. The Student *t* tests, Wilcoxon signed-rank tests, and the Mann-Whitney *U* tests with Bonferroni corrections were used for statistical comparisons. The non-parametric Kruskal-Wallis test was used to compare values between different groups. Correlation coefficients were calculated to assess whether there was a statistical dependence between the measured parameters. We have calculated that to detect a simple correlation ($r = .25$) with 80% power and a 5% significance level (two-tailed; $\alpha = .05$; $\beta = .2$), the required minimal sample size is approximately 123 cases. A *p* value lower than .05 was considered statistically significant. Statistical analyses were performed using StatSoft STATISTICA 13.1 software for Windows (StatSoft Inc.).

3 | RESULTS

The left atrial wall around the LAA orifice was the thickest at the anterior point (3.17 ± 1.41 mm, range: 1.12–8.91 mm), followed by the superior point (2.47 ± 1.00 mm, range: 0.34–5.52 mm), inferior

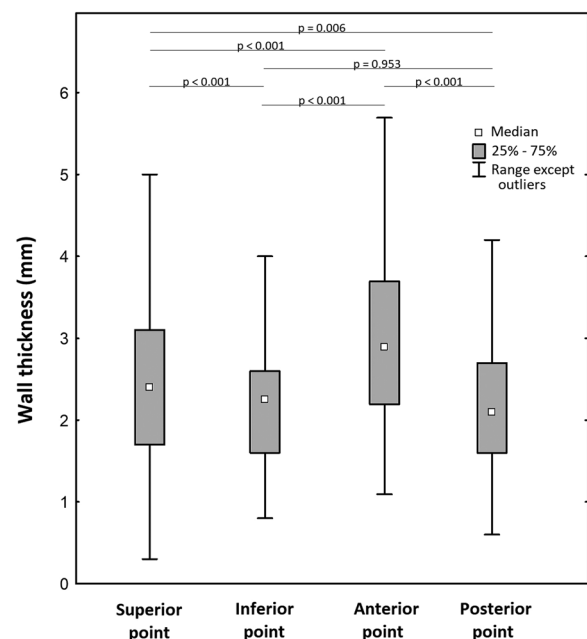


FIGURE 3 Box-and-Whiskers plot of median values for the wall thickness in different points around the left atrial appendage orifice. Wilcoxon signed-rank test with Bonferroni correction (significant *p* value level at .008)

TABLE 1 Results of obtained whole atrial wall thickness measurements with subgroups division

Measurement point	LAA body type			LAA orifice shape			Left atrial ridge		Left-sided pulmonary venous drainage "Classical"	
	All cases (n = 200)	Type I—cauliflower (n = 73)	Type II—chicken wing (n = 75)	Type III—arrowhead (n = 52)	Round (n = 110)	Oval (n = 90)	Presence (n = 116)	Absence (n = 84)	Left common pulmonary vein ostium (n = 17)	Left-sided pulmonary venous drainage (n = 183)
Superior point	2.47 ± 1.00	2.59 ± 0.94	2.17 ± 0.97	2.75 ± 1.05	2.25 ± 0.82	4.06 ± 0.72	2.51 ± 0.97	2.42 ± 1.06	2.44 ± 0.98	2.84 ± 1.22
Inferior point	2.22 ± 0.80	2.19 ± 0.86	2.28 ± 0.73	2.18 ± 0.84	2.18 ± 0.81	2.51 ± 0.69	2.26 ± 0.78	2.17 ± 0.84	2.22 ± 0.82	2.21 ± 0.63
Anterior point	3.17 ± 1.41	3.23 ± 1.38	3.23 ± 1.51	3.02 ± 1.33	3.04 ± 1.40	3.45 ± 1.52	3.10 ± 1.30	3.28 ± 1.56	3.18 ± 1.44	3.04 ± 1.12
Posterior point	2.22 ± 0.83	2.28 ± 0.89	2.18 ± 0.78	2.21 ± 0.83	2.15 ± 0.78	2.76 ± 0.95	2.23 ± 0.84	2.22 ± 0.82	2.24 ± 0.84	2.03 ± 0.67
							p Value	p Value	p Value	p Value
							.024	.432	.659	.854
							.000	.025	.048	.003
							.490	.409	.560	.869
							.231	.757	.994	.309

Note: Bold values denote statistical significance at the $p < .05$ level.

point (2.22 ± 0.80 mm, range: 0.83–5.35 mm), and posterior point (2.22 ± 0.83 mm, range: 0.61–5.43 mm) (Figure 3). The mean heart weight was 440.2 ± 97.4 g and was not significantly correlated with the tissue thickness in any measured point (all $r < .2$ and $p > .05$). There were no notable differences in measured thicknesses between sexes ($p > .05$). The thickness was not correlated with the donors' age or anthropometric features (weight, height, BMI) (all $r < .2$ and $p > .05$).

The most common LAA body shape was chicken wing (37.5%), followed by cauliflower (36.5%) and arrowhead (26.0%). A significant difference in the tissue thickness at the superior point was observed between different LAA types, where the chicken wing type was associated with the lowest thickness compared to the cauliflower and arrowhead shapes (Table 1, $p = .024$). No other significant differences connected with the LAA body type were observed (Table 1). The average LAA volume was 3.0 ± 2.1 ml and was not significantly correlated with the measured thicknesses (all $r < .2$ and $p > .05$).

The LAA orifice shape was described as round in 55.0% and oval in 45.0% of cases. In hearts with the oval LAA orifice, the atrial wall thickness was significantly thicker in all measured points than in specimens with round LAA orifice (Table 1). The calculated LAA orifice surface area was 1.4 ± 0.9 cm² and was negatively correlated with the tissue thickness in the anterior ($r = -.23$, $p = .001$) and posterior point ($r = -.28$, $p = .005$). The same negative correlations were observed between the LAA orifice anteroposterior diameter and the tissue thickness in both anterior and posterior points ($r = -.22$, $p = .004$ and $r = -.24$, $p = .001$, respectively).

The left lateral ridge was present in 58.0% of investigated hearts, and it did not affect the thickness of the wall around the LAA orifice (Table 1, $p > .05$). In only 8.5% of examined hearts, a variant in the left-sided pulmonary venous drainage was observed (i.e., single common left pulmonary vein ostium). The presence of common left pulmonary vein ostium also did not affect the thickness at the measured points (Table 1, $p > .05$).

A significant difference in the prevalence of additional structures on the endocardial surface (crevices, diverticula, trabeculae, or tissue bridges) was observed in different sectors around the LAA orifice. The inferior sector was the most affected by surface roughness (observed in 75.5% of hearts), followed by anterior (17.5%), superior (4.0%), and posterior sectors (1.5%) ($p = .001$); in the remaining cases, the endocardial surface was smooth (Figure 4).

4 | DISCUSSION

Although the current study is the first to investigate in detail the wall thickness around the LAA orifice, many previous studies have investigated atrial tissue thickness in different left atrium regions. Previous studies have shown that significant and clinically important variations exist for left atrial wall thickness at its different regions, which are commonly targeted during transcatheter ablation procedures.^{20–22} A great heterogeneity may be observed in tissue thickness with the values ranging from below 1–12 mm (mean:

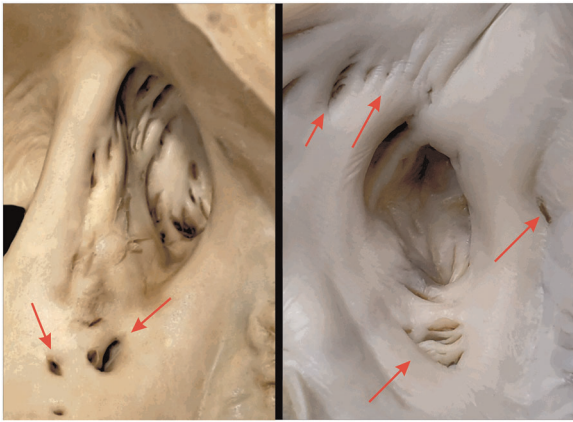


FIGURE 4 Photographs of cadaveric heart specimens showing left atrial appendage orifice with present additional structures on the endocardial surface (crevices, diverticula, trabeculae or tissue bridges) located in different sectors around the orifice (red arrows)

1–4 mm).²³ Nevertheless, there is no consensus regarding the general trends in the wall dimensions (anterior vs. posterior vs. roof vs. septal). The current study also showed diverse wall thickness around the LAA orifice, and the obtained values did not seem to differ significantly from measurements performed by other authors in different areas of the left atrium. Therefore, the tissue thickness in the proximity to the LAA orifice should be considered as a safe place for interventions, not differing significantly from other left atrial regions.

Electrophysiological conditions seem to change with wall thickness profile.²⁴ The general trend may be observed that patients predisposed to atrial arrhythmias have thicker tissue. Moreover, it was shown that thick and heterogeneous left atrial wall promotes atrial fibrillation recurrence after ablation.²³ The structure of the atrial wall influences the possibility of the creation of the transmural block and durable lesion; thus, it is an of arrhythmia recurrence after ablation.²⁵ Therefore, the atrial wall thickness might be an essential determinant of pathological tissue remodeling in patients with atrial arrhythmias and further a marker of response to ablation.²³ Finally, tissue thickness is a key factor responsible for procedural safety and the risk of perforation during the left atrial invasive procedures.²³

The current study shows that the thickest tissue might be observed at the anterior circumference of the LAA orifice. This might be explained by the anticipated presence of Bachmann's bundle fibers in this region.²⁶ Furthermore, we detected a significant association between the tissue thickness and the shape of the LAA orifice. The oval orifice is related to thicker tissue all around the LAA orifice. This might be important during LAA occlusion device implantation, where both oval shape and reduced surrounding tissue susceptibility to deformation may adversely affect the results of the procedure.⁹ On the other hand, bigger LAA orifices are correlated with the decreased tissue thickness in the anteroposterior axis. Another significant but difficult to explain observation of the current study is a significant narrowing of the tissue near the atrial roof in hearts with the chicken wing type LAA. Interestingly, despite its

regional diversity, the tissue thickness around the LAA orifice in the respective points is a constant parameter that is not affected by sex, age, or anthropometric parameters. Moreover, even the presence of the left lateral ridge or variants in the left-sided pulmonary venous drainage pattern does not influence the thickness around the LAA orifice. The knowledge we provide in this regard is a valuable hint for clinicians performing procedures within the LAA orifice area.

In the current study, endocardial surface roughness was observed around the LAA orifice. These structures should be identified as the embryological remnants of the pectinate muscles that extended from the LAA.²⁷ Such abrupt changes in myocardial thickness and fibers direction that are produced by the presence of the additional structures might act as an arrhythmogenic substrate.^{23,28} Moreover, the presence of additional crevices, recesses, and muscle bands can have a significant impact on transcatheter procedures within this region, as the unwanted structures might entrap the tip of a catheter and thus hinder the procedure. Also, energy adjustment might be necessary to reach the electrical block. An ablation index, that is a novel marker incorporating contact force, time, and power in a weighted formula to accurately estimate ablation lesion depth may be used for ablations within the left atrium, also within the LAA orifice area to achieve better lesion quality.^{29,30} However, operators should be aware, that endocardial surface roughness may decrease contact force being at the same time the sites of the reduced wall thickness.

Using imaging modalities that could analyze atrial tissue thickness and localize areas of increased as well as decreased wall thickness may improve the safety and effectiveness of ablation procedures.²³ Several available techniques can be used for this purpose. One of the available modality is cardiac magnetic resonance imaging; nevertheless, while this technique is suitable for atrial tissue characterization (e.g., fibrosis, scars, lesions, tissue remodeling), the spatial resolution of currently available magnetic resonance scanners is too low to precisely evaluate the thickness of the atrial tissue.³¹ Furthermore, transesophageal echocardiography and intracardiac echocardiography can be used to describe the wall of the left atrium; however, due to their invasive nature, they are mainly limited to the periprocedural period.^{32,33} On the other hand, transthoracic echocardiography that is widely used in clinical practice, does not provide adequate spatial resolution to allow the assessment of atrial tissue thickness.²³ Finally, cardiac computed tomography is considered the most optimal and accessible technique for assessing the structure of the left atrial wall that allows reconstructing the whole atrium with the fine resolution.³⁴ Almost all anatomical information about the LAA may be provided by high-resolution and high-quality contrast enhanced electrocardiographically-gated cardiac computed tomography. The LAA shape and size may be easily assessed using standard imaging and 3D reconstructions.⁴ Moreover the left atrial wall thickness may also be easily measured using computed tomography imaging that largely reflects the real anatomy of this region.³⁵ Therefore, the computed tomography plays a key role in the periprocedural planning and postprocedural evaluation during the LAA device implantations and wide range of interventions targeted to LAA.³⁶

There are several limitations to this study that should be noticed. The major one is that this study was performed on autopsied material preserved in paraformaldehyde solution. Therefore, slight changes to the size and shape of the studied specimens due to the fixation process may occur. However, our previous studies have proved that a paraformaldehyde solution did not cause significant changes in cardiac dimensions.³⁷ Also, because the post-mortem tissue was investigated, we were unable to evaluate the behavior and dimensional changes of left atrial wall components during the cardiac cycle. Furthermore, only hearts from healthy donors were investigated. Hence our results might not fully reflect the morphology attributed to patients with structural heart diseases and arrhythmias. As left atrial wall structural remodeling occurs with prolonged episodes of atrial fibrillation, further studies on specimens with a history of arrhythmias should be conducted. Moreover, measurements were performed only in four selected points that may not fully cover the structure of the left atrial wall around the entire LAA orifice circumference. Finally, only the whole atrial wall tissue was measured with no further subdivision to tissue layers. Despite these limitations, we believe that this study has provided significant insight into the morphometrical characteristics of the left atrium and the LAA.

5 | CONCLUSIONS

Significant heterogeneity in the left atrial wall thickness around the LAA orifice is observed, with the thickest wall observed at the mitral valve annulus point. At its thinnest point, the wall around the LAA orifice can measure below 0.5 mm. When considering the respective points, the tissue thickness around the LAA orifice is a quite conservative parameter that is not affected by sex, age, or anthropometric parameters, as well as the presence of the left lateral ridge and left-sided pulmonary veins variants. Similarly, the LAA body shape has no major impact on the tissue around the LAA orifice, except for the superior point, for which the chicken wing type was associated with the lowest thickness. Both the LAA orifice shape (oval vs. round) and size (dimension and area) have a significant impact on the tissue thickness around the LAA orifice. Endocardial surface roughness is commonly present in the inferior pole of the LAA orifice (75% of cases), while they are much less prevalent in other sectors around the orifice.

DATA AVAILABILITY STATEMENT

The data that support the findings of this study are available from the corresponding author upon reasonable request.

REFERENCES

- Dudkiewicz D, Słodowska K, Jasińska KA, Dobrzynski H, Hołda MK. The clinical anatomy of the left atrial structures used as landmarks in ablation of arrhythmogenic substrates and cardiac invasive procedures. *Transl Res Anat.* 2021;23:100102. <https://doi.org/10.1016/j.tria.2020.100102>
- Sylva M, Van den Hoff MJB, Moorman AFM. Development of the human heart. *Am J Med Genet, Part A.* 2014;164A:1347-1371. <https://doi.org/10.1002/ajmg.a.35896>
- Whiteman S, Saker E, Courant V, et al. An anatomical review of the left atrium. *Transl Res Anat.* 2019;17:100052. <https://doi.org/10.1016/j.tria.2019.100052>
- Beigel R, Wunderlich NC, Ho SY, Arsanjani R, Siegel RJ. The left atrial appendage: anatomy, function, and noninvasive evaluation. *JACC Cardiovasc Imaging.* 2014;7(12):1251-1265. <https://doi.org/10.1016/j.jcmg.2014.08.009>
- Patti G, Pengo V, Marcucci R, et al. The left atrial appendage: from embryology to prevention of thromboembolism. *Eur Heart J.* 2017;38(12):877-887. <https://doi.org/10.1093/eurheartj/ehw159>
- Barbero U, Ho SY. Anatomy of the atria: a road map to the left atrial appendage. *Herzschrittmachertherapie + Elektrophysiologie.* 2017;28:347-354. <https://doi.org/10.1007/s00399-017-0535-x>
- Baman JR, Mansour M, Heist EK, Huang DT, Biton Y. Percutaneous left atrial appendage occlusion in the prevention of stroke in atrial fibrillation: a systematic review. *Heart Fail Rev.* 2018;23:191-208. <https://doi.org/10.1007/s10741-018-9681-4>
- Reddy VY, Holmes D, Doshi SK, Neuzil P, Kar S. Safety of percutaneous left atrial appendage closure: results from the watchman left atrial appendage system for embolic protection in patients with AF (PROTECT AF) clinical trial and the continued access registry. *Circulation.* 2011;123:417-424. <https://doi.org/10.1161/CIRCULATIONAHA.110.976449>
- Dieker W, Behnes M, Fastner C, et al. Impact of left atrial appendage morphology on thrombus formation after successful left atrial appendage occlusion: assessment with cardiac-computed-tomography. *Sci Rep.* 2018;8(1):1670. <https://doi.org/10.1038/s41598-018-19385-z>
- Masci A, Barone L, Dedè L, et al. The impact of left atrium appendage morphology on stroke risk assessment in atrial fibrillation: a computational fluid dynamics study. *Front Physiol.* 2019;9:9. <https://doi.org/10.3389/fphys.2018.01938>
- Di Biase L, Burkhardt JD, Mohanty P, et al. Left atrial appendage: an underrecognized trigger site of atrial fibrillation. *Circulation.* 2010;122(2):109-118. <https://doi.org/10.1161/CIRCULATIONAHA.109.928903>
- Hocini M, Shah AJ, Nault I, et al. Localized reentry within the left atrial appendage: arrhythmogenic role in patients undergoing ablation of persistent atrial fibrillation. *Hear Rhythm.* 2011;8(12):1853-1861. <https://doi.org/10.1016/j.hrthm.2011.07.013>
- Alturki A, Huynh T, Dawas A, et al. Left atrial appendage isolation in atrial fibrillation catheter ablation: A meta-analysis. 2018. <https://doi.org/10.1002/joa3.12095>
- Kawamura M, Scheinman MM, Lee RJ, Badhwar N. Left atrial appendage ligation in patients with atrial fibrillation leads to a decrease in atrial dispersion. *J Am Heart Assoc.* 2015;4(5):e001581. <https://doi.org/10.1161/JAHA.114.001581>
- Cabrera JA, Ho SY, Climent V, Sánchez-Quintana D. The architecture of the left lateral atrial wall: a particular anatomic region with implications for ablation of atrial fibrillation. *Eur Hear J.* 2008;29(3):356-362. <https://doi.org/10.1093/eurheartj/ehm606>
- Nishimura M, Lupercio-Lopez F, Hsu JC. Left atrial appendage electrical isolation as a target in atrial fibrillation. *JACC Clin Electrophysiol.* 2019;5(4):407-416. <https://doi.org/10.1016/j.jacep.2019.02.009>
- Panikker S, Jarman JW, Virmani R, et al. Left atrial appendage electrical isolation and concomitant device occlusion to treat persistent atrial fibrillation: a first-in-human safety, feasibility, and efficacy study. *Circ Arrhythm Electrophysiol.* 2016;9(7):e003710. <https://doi.org/10.1161/CIRCEP.115.003710>
- Słodowska K, Szczepanek E, Dudkiewicz D, et al. Morphology of the left atrial appendage—introduction of a new simplified shape-based classification system. *Hear Lung Circ.* 2020;30(7):1014-1022.

19. Piątek-Koziej K, Hołda J, Tyrak K, et al. Anatomy of the left atrial ridge (coumadin ridge) and possible clinical implications for cardiovascular imaging and invasive procedures. *J Cardiovasc Electrophysiol*. 2020;31(1):220-226. <https://doi.org/10.1111/jce.14307>
20. Tan HW, Wang XH, Shi HF, Zhou L, Gu JN, Liu X. Left atrial wall thickness: anatomic aspects relevant to catheter ablation of atrial fibrillation. *Chin Med J (Engl)*. 2012;125(1):12-15. <https://doi.org/10.3760/cma.j.issn.0366-6999.2012.01.003>
21. Platonov PG, Ivanov V, Ho SY, Mitrofanova L. Left atrial posterior wall thickness in patients with and without atrial fibrillation: data from 298 consecutive autopsies. *J Cardiovasc Electrophysiol*. 2008;19(7):689-692. <https://doi.org/10.1111/j.1540-8167.2008.01102.x>
22. Hall B, Jeevanantham V, Simon R, Filippone J, Vorobiof G, Daubert J. Variation in left atrial transmural wall thickness at sites commonly targeted for ablation of atrial fibrillation. *J Interv Card Electrophysiol*. 2006;17(2):127-132. <https://doi.org/10.1007/s10840-006-9052-2>
23. Whitaker J, Rajani R, Chubb H, et al. The role of myocardial wall thickness in atrial arrhythmogenesis. *Europace*. 2016;18(12):1758-1772. <https://doi.org/10.1093/europace/euw014>
24. Nakamura K, Funabashi N, Uehara M, et al. Left atrial wall thickness in paroxysmal atrial fibrillation by multislice-CT is initial marker of structural remodeling and predictor of transition from paroxysmal to chronic form. *Int J Cardiol*. 2011;148(2):139-147. <https://doi.org/10.1016/j.ijcard.2009.10.032>
25. Inoue J, Skanes AC, Gula LJ, Drangova M. Effect of left atrial wall thickness on radiofrequency ablation success. *J Cardiovasc Electrophysiol*. 2016;27(11):1298-1303. <https://doi.org/10.1111/jce.13065>
26. Van Campenhout MJ, Yaksh A, Kik C, et al. Bachmann's bundle a key player in the development of atrial fibrillation? *Circ Arrhythmia Electrophysiol*. 2013;6(5):1041-1046. <https://doi.org/10.1161/CIRCEP.113.000758>
27. Hołda MK, Koziej M, Hołda J, et al. Anatomic characteristics of the mitral isthmus region: the left atrial appendage isthmus as a possible ablation target. *Ann Anat*. 2017;210:103-111. <https://doi.org/10.1016/j.aanat.2016.11.011>
28. Klos M, Calvo D, Yamazaki M, et al. Atrial septopulmonary bundle of the posterior left atrium provides a substrate for atrial fibrillation initiation in a model of vagally mediated pulmonary vein tachycardia of the structurally normal heart. *Circ Arrhythm Electrophysiol*. 2008;1(3):175-183. <https://doi.org/10.1161/CIRCEP.107.760447>
29. Das M, Loveday JJ, Wynn GJ, et al. Ablation index, a novel marker of ablation lesion quality: prediction of pulmonary vein reconnection at repeat electrophysiology study and regional differences in target values. *Europace*. 2017;19(5):775-783. <https://doi.org/10.1093/europace/euw105>
30. Santoro F, Metzner A, Brunetti ND, et al. Left atrial anterior line ablation using ablation index and inter-lesion distance measurement. *Clin Res Cardiol*. 2019;108:1009-1016. <https://doi.org/10.1007/s00392-019-01428-8>
31. Chen YA, Nguyen ET, Dennie C, et al. Computed tomography and magnetic resonance imaging of the coronary sinus: anatomic variants and congenital anomalies. *Insights Imaging*. 2014;5(5):547-557. <https://doi.org/10.1007/s13244-014-0330-8>
32. López-Candales A, Grewal H, Katz W. The importance of increased interatrial septal thickness in patients with atrial fibrillation: a transesophageal echocardiographic study. *Echocardiography*. 2005;22(5):408-414. <https://doi.org/10.1111/j.1540-8175.2005.04088.x>
33. Enriquez A, Saenz LC, Rosso R, et al. Use of intracardiac echocardiography in interventional cardiology working with the anatomy rather than fighting it. *Circulation*. 2018;137(21):2278-2294. <https://doi.org/10.1161/CIRCULATIONAHA.117.031343>
34. Dewland TA, Wintermark M, Vaysman A, et al. Use of computed tomography to identify atrial fibrillation associated differences in left atrial wall thickness and density. *PACE—Pacing Clin Electrophysiol*. 2013;36(1):55-62. <https://doi.org/10.1111/pace.12028>
35. Beinart R, Abbara S, Blum A, et al. Left atrial wall thickness variability measured by CT scans in patients undergoing pulmonary vein isolation. *J Cardiovasc Electrophysiol*. 2011;22(11):1232-1236. <https://doi.org/10.1111/j.1540-8167.2011.02100.x>
36. Korsholm K, Berti S, Iriart X, et al. Expert recommendations on cardiac computed tomography for planning transcatheter left atrial appendage occlusion. *JACC Cardiovasc Interv*. 2020;13(3):277-292. <https://doi.org/10.1016/j.jcin.2019.08.054>
37. Hołda MK, Klimek-Piotrowska W, Koziej M, Piątek K, Hołda J. Influence of different fixation protocols on the preservation and dimensions of cardiac tissue. *J Anat*. 2016;229(2):334-340. <https://doi.org/10.1111/joa.12469>

How to cite this article: Słodowska K, Hołda J, Dudkiewicz D, et al. Thickness of the left atrial wall surrounding the left atrial appendage orifice. *J Cardiovasc Electrophysiol*. 2021;32:2262-2268. <https://doi.org/10.1111/jce.15157>